CHAPTER 4

RESULTS AND DISCUSSIONS

In 1996, Mustafa *et. al.*[112] reported that the $CHCl_3$ extract of *Kaempferia galanga* Linn. relaxed the smooth muscles of rat aorta. In the light of the above finding, chemical and pharmacological studies were performed on this plant with the objectives to isolate and identify the compound (or compounds) responsible for the vasorelaxant activity.

This study was divided into three parts:

a) the bioassay-guided and chemical study of the CH_2Cl_2 extract,

b) the chemical study of the pet. ether extract with emphasis on its volatile components since this plant is also used in preparation of ointments and liniments (refer chapter 1), and

c) the study of the mechanisms of the vasorelaxant action of the bioactive compound(s).

4.1 BIOASSAY-GUIDED STUDY OF THE CH_2Cl_2 EXTRACT OF *KAEMPFERIA GALANGA* LINN.

The dried rhizomes of *Kaempferia galanga* Linn. were extracted with CH_2Cl_2 using soxhlet extractor and yielded 2.92% of the crude CH_2Cl_2 extract which was then subjected to the brine shrimp lethality assay (ED_{50} = 7.92 μg ml^{-1}) and was screened for vasorelaxant activity. Since both tests showed considerable activities, a bioassay-guided fractionation was performed on the extract in order to isolate the bioactive compound (or mixture of compounds) contributing to the vasorelaxant activity of the smooth muscles of rat aorta, as shown in the flowchart in figure 4.1.

FIGURE 4.1 SCHEMATIC PROCEDURE OF ISOLATION OF THE CHEMICAL CONSTITUENTS FROM *KAEMPFERIA GALANGA* LINN.

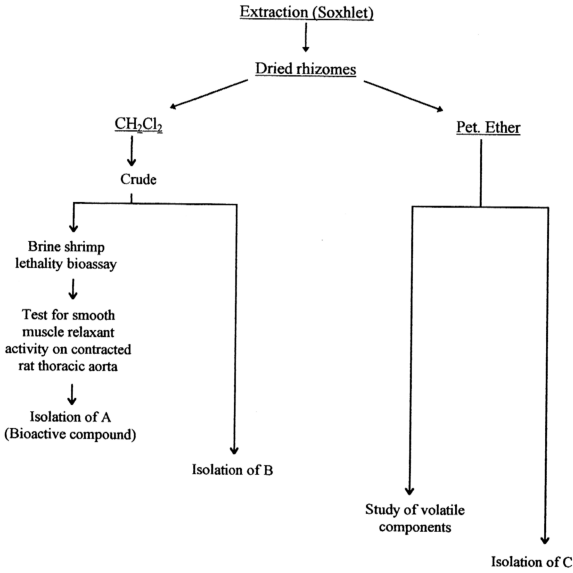

The bioactive compound was isolated as colourless oil and labelled compound A. This compound had an R_f value of 0.55 on tlc with solvent system pet. ether : ethyl acetate (90:10). Another compound also obtained from the CH_2Cl_2 extract was named compound B. This compound crystallized out from the crude CH_2Cl_2 extract under cold condition and represented 0.28% of the extract. Compound B was recrystallized from CH_2Cl_2 and purified as white needles with melting point of 176-177°C.

Vasorelaxant action of compound A on smooth muscles of rat aorta were compared to those of other structurally similar compounds. Consequently, results obtained were analyzed and the structure-activity relationship of the vasorelaxant activity of these compounds on the smooth muscles of rat aorta was proposed.

4.1.1 Brine shrimp lethality bioassay on crude CH_2Cl_2 extract

This bioassay was designed as an inexpensive, rapid and simple 'bench-top' assay to monitor the bioactive plant extracts during fractionation and during preliminary screening. This method was found to be suitable for assessing *in vivo* lethality of crude or pure compounds on simple zoological organisms[113,114].

Ten different concentrations of the crude CH_2Cl_2 extract were tested, and each concentration was examined in triplicate. One set of control was done by excluding the test sample. The data was analysed using the Finney computer program which was obtained from Professor Jerry McLaughlin, Purdue University, Indiana 47907, U.S.A. for the determination of ED_{50} values with 95% confidence

intervals. ED_{50} values greater than 20 μg ml^{-1} for pure compounds were considered inactive.

Table 4.1 shows the results of the preliminary screening of the CH_2Cl_2 extract from *Kaempferia galanga* Linn. for biological activity at different concentrations using the brine shrimp lethality bioassay. Analysis of the data using Finney computer program showed that this extract exhibited potent bioactivity with ED_{50} value of 7.92 μg ml^{-1}. The extract was subsequently screened for vasorelaxant activity on the precontracted rat thoracic aorta.

4.1.2 Screening of crude CH_2Cl_2 extract for antihypertensive activity

Initial experiments were carried out to screen the crude CH_2Cl_2 extract for antihypertensive activity in anaesthetized rats. The concentrations of the crude extract used in this experiment were 100 mg ml^{-1}, 33 mg ml^{-1} and 10 mg ml^{-1}. As seen in figure 4.2, administration of the crude extract induced a dose-related reduction of mean arterial pressure, MAP, (130 ± 5 mm Hg), which reached a maximal effect after 5-10 minutes of injection; i.e. increasing the concentration of the crude extract further decreased the blood pressure of the rats. The result of this experiment demonstrated that this crude extract showed an antihypertensive property since it effectively lowered the MAP in anaesthetized rats.

TABLE 4.1 PRELIMINARY SCREENING FOR BIOLOGICAL ACTIVITY OF CRUDE CH_2Cl_2 EXTRACT USING THE BRINE SHRIMP LETHALITY BIOASSAY

Sample	Number of shrimps																	
	Concentration / μg ml^{-1}																	
	0.5						5						6					
	I		II		III		I		II		III		I		II		III	
	s	d	s	d	s	d	s	d	s	d	s	d	s	d	s	d	s	d
CH_2Cl_2 extract	10	0	10	0	10	0	10	0	10	0	10	0	7	3	5	5	6	4
Control	10	0	10	0	10	0	10	0	10	0	10	0	10	0	10	0	10	0

Sample	Number of shrimps																	
	Concentration / μg ml^{-1}																	
	7						8						9					
	I		II		III		I		II		III		I		II		III	
	s	d	s	d	s	d	s	d	s	d	s	d	s	d	s	d	s	d
CH_2Cl_2 extract	7	3	5	5	5	5	9	1	7	3	5	5	3	7	3	7	3	7
Control	10	0	10	0	10	0	10	0	10	0	10	0	10	0	10	0	10	0

Sample	Number of shrimps																	
	Concentration / μg ml^{-1}																	
	10						100						1000					
	I		II		III		I		II		III		I		II		III	
	s	d	s	d	s	d	s	d	s	d	s	d	s	d	s	d	s	d
CH_2Cl_2 extract	0	10	0	10	0	10	0	10	0	10	0	10	0	10	0	10	0	10
Control	10	0	10	0	10	0	10	0	10	0	10	0	10	0	10	0	10	0

s = survived, d = dead

FIGURE 4.2 EFFECT OF THE CH_2Cl_2 EXTRACT OF *KAEMPFERIA GALANGA* LINN. ON THE MEAN ARTERIAL PRESSURE OF ANAESTHETIZED RATS

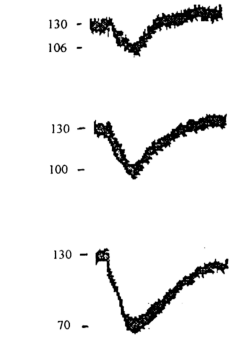

4.1.3 Isolation of compound A

The crude CH_2Cl_2 extract was put through precipitation process by the addition of 1090 ml of pet. ether to 98 g of the crude extract. The filtrate was separated from the mother liquor by filtration with vacuum pump. The mother liquor (KDNP) obtained was dark brown in colour, quite viscous and constituted 90.6% of the crude CH_2Cl_2 extract. It was screened for vasorelaxant activity on smooth muscle of isolated rat thoracic aorta and a positive result was obtained.

The steps taken to detect and isolate the active compound are depicted in figure 4.3. KDNP was put through column chromatography with a mixture of CH_2Cl_2:CH_3OH as the eluant at increasing polarity. Nine fractions were obtained and fraction 2 (100% CH_2Cl_2) exhibited vasorelaxant activity on isolated rat thoracic aorta. The latter was further separated using preparative tlc with pet. ether : ethyl acetate (95:5) as solvent system. Three fractions were obtained and fraction 2 (R_f = 0.62) exhibited a positive result. Further separation was done on fraction 2 (R_f = 0.62) using preparative thin-layer chromatography with pet. ether : ethyl acetate (92:8) as eluant. Six fractions were obtained and four fractions showed activity with the third fraction (R_f = 0.58) giving the maximum relaxation. The mass chromatograms of the first four active fractions are shown in figure 4.4 and table 4.2. These findings could suggest that ethyl cinnamate might be the component contributing to the vasorelaxant activity of contracted smooth muscle of the rat aorta since in all the four fractions that were active, it was present in considerable amount. In fraction 3, which was the most active fraction, ethyl cinnamate was the major compound identified. Fraction 2 (R_f = 0.75) was subjected to further

FIGURE 4.3 DETECTION AND ISOLATION OF THE BIOACTIVE COMPOUND OF *KAEMPFERIA GALANGA* LINN.

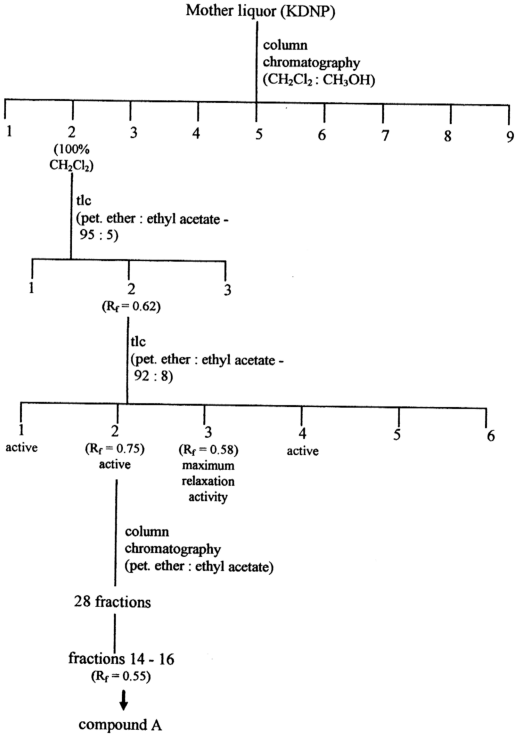

FIGURE 4.4 GAS CHROMATOGRAMS OF THE ACTIVE FRACTIONS 1, 2, 3 AND 4, RESPECTIVELY

Fraction 1

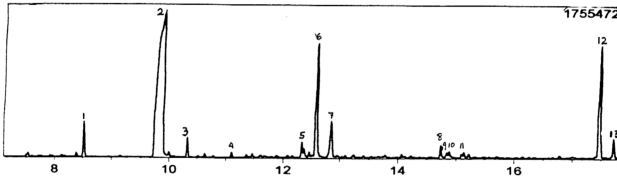

Fraction 2

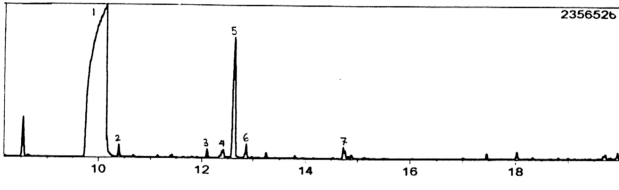

Fraction 3

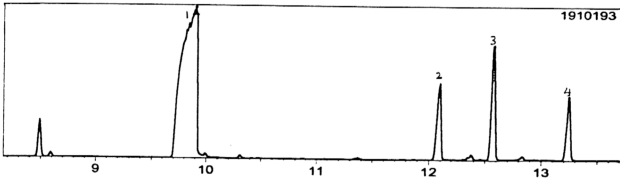

Fraction 4

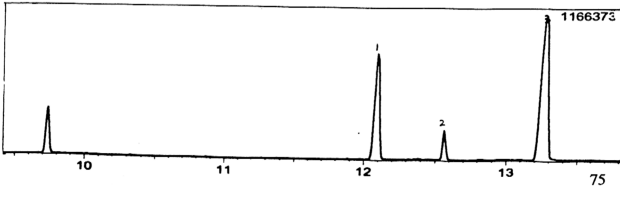

TABLE 4.2 TABLES SHOWING THE CHEMICAL CONSTITUENTS OF THE ACTIVE FRACTIONS 1, 2, 3 AND 4, RESPECTIVELY, AS ELUCIDATED FROM THE GC-MS

Fraction 1

No.	Rt	Mol. Formula	%	Name
1	8.508	$C_{11}H_{12}O_2$	2.39	Ethyl cinnamate
2	9.875	$C_{11}H_{12}O_2$	40.63	Ethyl cinnamate
3	10.317	$C_{11}H_{22}O$	1.17	Undecanone
4	11.092	$C_{12}H_{14}O_2$	0.36	Isopropyl cinnamate
5	12.317	$C_{15}H_{22}N_2$	1.14	Dicyclohexylpropanedinitrile
6	12.583	$C_{10}H_{16}O_2$	10.27	Dipentene dioxide
7	12.842	$C_9H_{18}O_2$	3.87	9-Hydroxy-2-nonanone
8	14.717	$C_{10}H_{16}O_2$	0.91	(z)-2,7-Octadien-1-yl acetate
9	14.825	$C_{10}H_{18}O_2$	0.47	Ethyl cyclohexyl acetate
10	14.867	$C_{11}H_{22}O$	0.57	*cis*-11-Tetradecenyl acetate
11	15.117	$C_{17}H_{34}O$	0.39	2-Heptadecanone
12	17.467	$C_{11}H_{18}O$	10.63	4-Methyl isopulegone
13	17.700	$C_{10}H_{19}N$	1.57	Camphidine

Fraction 2

No.	Rt	Mol.Formula	%	Name
1	10.133	$C_{11}H_{12}O_2$	>40.00	Ethyl cinnamate
2	10.375	$C_{11}H_{22}O$	1.54	Undecanone
3	12.083	$C_{12}H_{14}O_3$	1.21	Ethyl *p*-methoxycinnamate
4	12.400	$C_{10}H_{16}O_2$	1.03	*trans,trans*-Octa-2,4-dienyl acetate
5	12.617	$C_{11}H_{20}O$	28.25	10-Undecyn-1-ol
6	12.850	$C_{11}H_{22}O$	2.60	Undecanone
7	14.717	$C_{10}H_{16}O_2$	1.68	Dipentene dioxide
8	19.933	$C_{11}H_{12}O_2$	1.09	Ethyl cinnamate

Fraction 3

No.	Rt	Mol. Formula	%	Name
1	9.900	$C_{11}H_{12}O_2$	59.59	Ethyl cinnamate
2	12.092	$C_{12}H_{14}O_3$	9.09	Ethyl *p*-methoxycinnamate
3	12.567	$C_{10}H_{16}O_2$	12.18	Dipentene dioxide
4	13.2422	$C_{12}H_{14}O_3$	4.04	Ethyl *p*-methoxycinnamate

Fraction 4

No.	Rt	Mol. Formula	%	Name
1	12.092	$C_{12}H_{14}O_3$	23.87	Ethyl *p*-methoxycinnamate
2	12.558	$C_{10}H_{16}O_2$	5.04	(z)-2,7-Octadien-1-yl acetate
3	13.283	$C_{12}H_{14}O_3$	47.68	Ethyl *p*-methoxycinnamate

separation since it contained the most amount of sample. This fraction was subjected to column chromatography with pet. ether : ethyl acetate (with increasing polarity) as eluant. Twenty eight fractions were obtained. From the tlc, it was shown that fractions 14 to 16 consisted of the same single compound with R_f value of 0.55. These fractions were grouped together and labelled compound A. Pharmacological tests showed that compound A exhibited marked vasorelaxant activity on contracted smooth muscle of isolated the rat thoracic aorta.

4.1.3.1 *Vasorelaxant activity of compound A*

(a) Effect of compound A on the contractions induced by high K^+ concentration (high K^+) and phenylephrine (PE) in endothelium intact rat aorta.

In rat aorta, addition of high K^+ caused a tonic contraction whilst addition of PE caused an initial phasic contraction followed by a tonic contraction (diagram 4.1)[112]. Contractions induced by high K^+ were due to membrane depolarization, which activated L-type (long lasting) voltage-dependent Ca^{2+} channel (VDC) and thus permitted Ca^{2+} entry[85]. In addition to voltage-dependent Ca^{2+} channel, PE activated receptor-operated non-selective Ca^{2+} channels (ROC) to induce the sustained contraction. The high K^+- and PE-induced contractions reached maximum in 15 and 10 minutes, respectively, and both contractions were maintained for at least 30 minutes.

In this experiment, the rat aorta was precontracted with 80 mM of high K^+ or 0.1 μM PE. When the contractions to either spasmogens reached maximum,

DIAGRAM 4.1 TONIC AND PHASIC CONTRACTIONS OF THE RAT AORTA

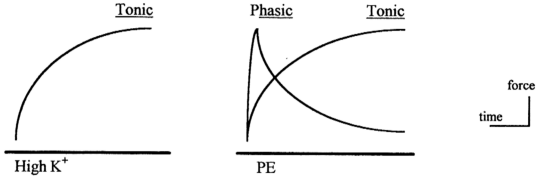

The diagram above shows the different types of contractions induced by high K^+ and PE. In Ca^{2+}-free solution, only the phasic phase is observed.

cumulative concentrations of compound A were added to the bath every ten minutes. As shown in figure 4.5, the cumulative applications of compound A inhibited the sustained contractions induced by both spasmogens. Compound A dose-dependently inhibited the sustained contractions to high K^+ and PE with IC_{50} values of 0.30 mM and 0.38 mM, respectively.

(b) Time course of the inhibitory effect of compound A on the contractions induced by high K^+ and PE in endothelium intact rat aorta.

The isolated rat aorta was precontracted with 80 mM or 0.1 μM PE. When the contractions to either spasmogens became maximum, a single concentration of compound A (based on the IC_{50} value) was added to the bath. As shown in figure 4.6, compound A inhibited the contraction to high K^+ at a faster rate than to PE. Ten minutes after the addition of compound A, contractions induced by high K^+ was diminished by 80.92 ± 6.84 % ($n = 5$) but PE-induced contraction was only reduced by 64.60 ± 6.07 % ($n = 4$).

FIGURE 4.5 EFFECT OF COMPOUND A ON THE CONTRACTIONS INDUCED BY HIGH K^+ AND PE IN ENDOTHELIUM INTACT RAT AORTA

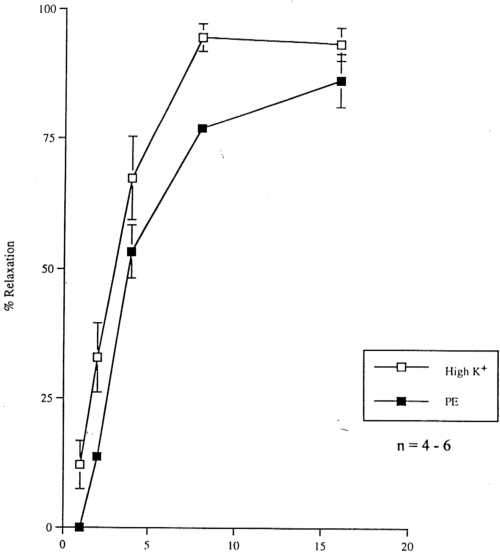

FIGURE 4.6 TIME COURSE OF THE INHIBITORY EFFECT OF COMPOUND A ON THE CONTRACTIONS INDUCED BY HIGH K^+ AND PE IN ENDOTHELIUM INTACT RAT AORTA

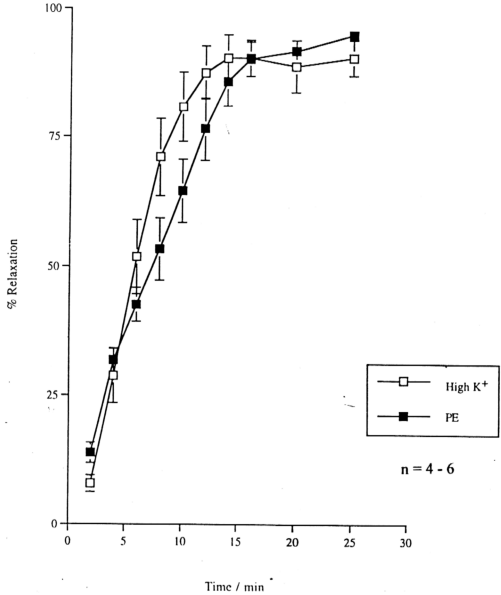

4.1.4 Structural elucidation and determination of compounds isolated from the CH_2Cl_2 extract of *Kaempferia galanga* Linn.

4.1.4.1 *Compound A*

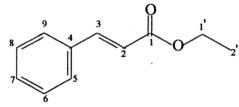

83

Compound A was obtained as a colourless oil. It's UV spectrum revealed typical benzenoid absorption band at 276.6 nm (log ε 4.39) and *K* band at 217.3 nm (4.12), indicating a highly conjugated unsaturated aromatic system.

The mass spectrum (figure 4.7) showed a molecular ion peak at m/z = 176, thus giving the possibility of the molecular formula to be $C_{11}H_{12}O_2$. Other significant fragmentations revealed by the mass spectrum were m/z = 148, 131 (100%; base peak), 103 and 77. Scheme 4.1 illustrates the proposed fragmentations underwent by compound A in the mass spectrum. The first step of the scheme involved a hydrogen transfer to the carbonyl oxygen in a process known as the Mc Lafferty rearrangement (carbonyl compounds with a hydrogen on their γ carbon undergo this rearrangement)[115], which simultaneously eliminated an ethylene unit. The following loss of a hydroxyl radical gave rise to the base peak at m/z = 131, and

FIGURE 4.7 MASS SPECTRUM OF COMPOUND A

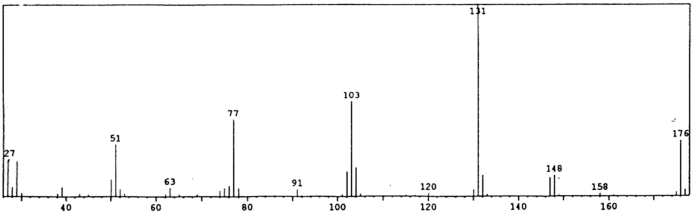

SCHEME 4.1 THE MASS FRAGMENTATION PATTERNS OF COMPOUND A

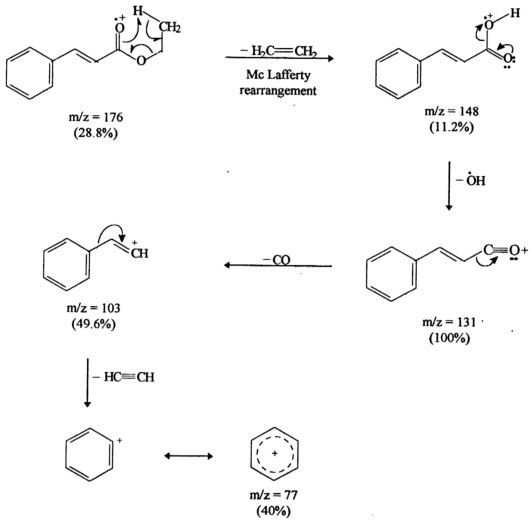

subsequent losses of a carbonyl unit and an acetylene molecule produced a C_6H_7 ion at m/z = 77.

The IR spectrum of compound A (figure 4.8) revealed bands between 3063 cm^{-1} and 2903 cm^{-1} which corresponded to the stretching vibrations of the phenyl C–H and alkyl C–H bonds, respectively. Weak bands at 1956 and 1883 cm^{-1} represented weak combinations and overtones for the aromatic ring. In addition, the strong band at 1705 cm^{-1} could be assigned to the stretching vibrations of the conjugated C=O bond (i.e. α,β-unsaturated ester conjugated with an aromatic ring[68]), while those at 1639 and 1450 cm^{-1} could be due to C=C bond stretching of the benzene ring and alkene. Multiple bands could be observed between 1369 and 1278 cm^{-1} and these might be assigned to the C–O stretching of the ester moiety (i.e. C–C(=O)–O). Furthermore, the peak at 1200 cm^{-1} could be due to the in-plane bending of the aromatic ring. Finally, the signal at 1041 cm^{-1} might be attributable to the asymmetric stretching of the O–C bond of the ester (i.e. O–C–C).

Figure 4.9 showed the ^{1}HNMR spectrum of compound A. It could be deduced from this spectrum that a triplet corresponding to three protons at 1.28 ppm belonged to a methyl group adjacent to an ethyl. The quartet at 4.21 ppm could be assigned to two protons of an ethyl group, adjacent to the methyl group, and were highly deshielded by the neighbouring oxygen atom.

An AX system could be observed for the two ethylene protons adjacent to the aromatic ring where $\Delta\nu/J \sim 31$. Appearance of a doublet at 6.38 ppm (1H, d, J_2 =

FIGURE 4.8 IR SPECTRUM OF COMPOUND A

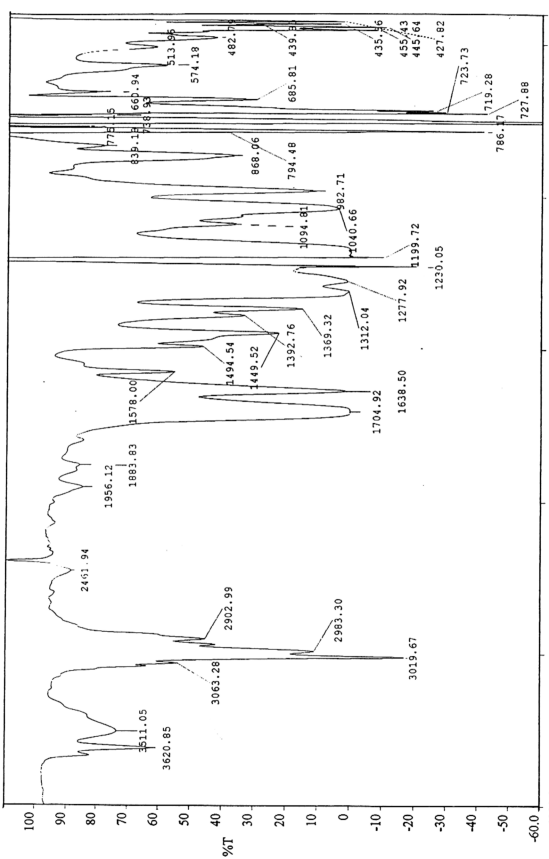

FIGURE 4.9 ^{1}HNMR SPECTRUM OF COMPOUND A

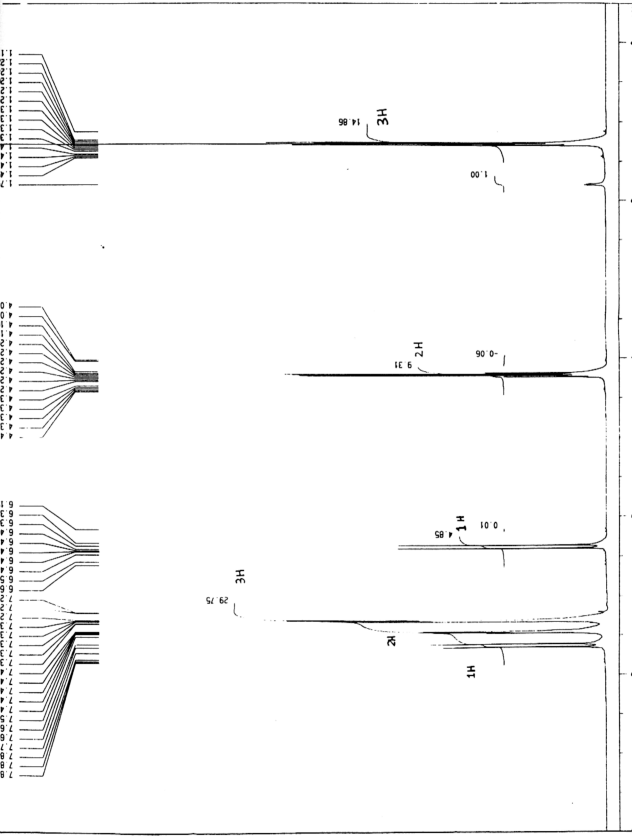

16.1 Hz) was indicative of the proton at C-2, while C-3 proton resonated further downfield at 7.63 ppm (1H, d, J_3 = 16.1 Hz). This could be explained by the fact that the β proton of an α,β-unsaturated ester is further downfield than the α proton because delocalization of electrons results in a lower electron density at the β proton, which, thus experiences a deshielding effect[65]. This reversible process of electron delocalization is illustrated diagramatically below. Furthermore, $J_{AX} \approx 16$ Hz indicated that the two ethylene protons were in the *trans* conformation.

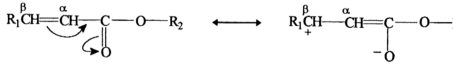

A multiplet in the range of 7.31 - 7.47 ppm (5H, m, H-5 - H-9) were attributable to the protons on the benzene ring.

The ^{13}CNMR spectrum (figure 4.10) exhibited a upfield signal at 14.24 ppm attributable to the methyl carbon. The ethyl carbon adjacent to the oxygen atom gave rise to downfield peak at 60.39 ppm due to the deshielding effect of the neighbouring oxygen atom. The two sp^2 carbons of ethylene, ie. C-2 and C-3, gave signals at 118.23 and 144.48 ppm, respectively. The latter experienced a deshielding effect from the C=O of the ester moiety due to its β position from the group. Peaks at positions 127.95 - 134.41 ppm were indicative of the sp^2 carbons of the benzene ring. The *sp* carbon of the ester showed a signal at 166.88 ppm.

FIGURE 4.10 ^{13}CNMR SPECTRUM OF COMPOUND A

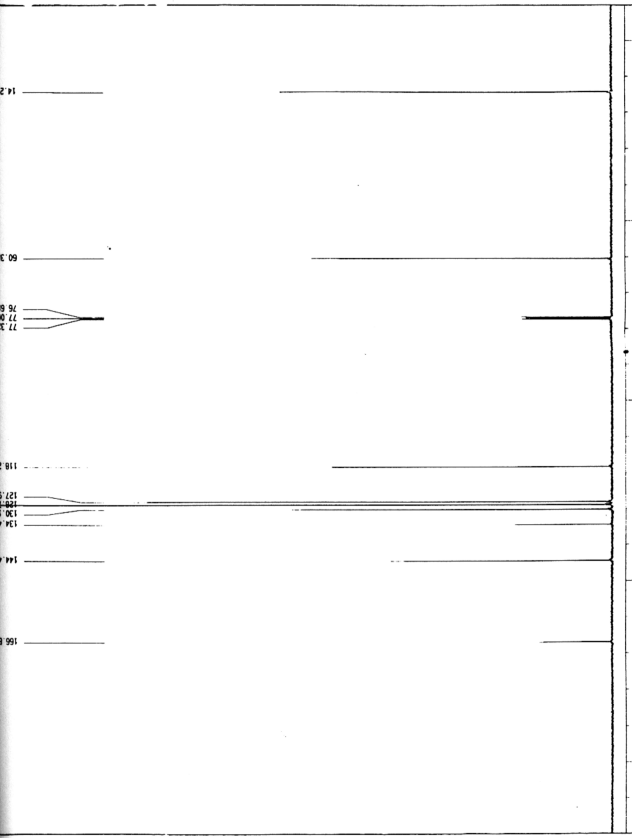

Figure 4.11 showed the DEPT (distortionless enhancement by polarisation transfer) spectrum of compound A. This is a useful technique to distinguish C, CH, CH_2 and CH_3 signals. Peaks shown after the $90°_y$ pulses are attributable to CH of the ethylene and aromatic ring. Peaks shown after the 135° delay are assigned to CH (up) of the ethylene and aromatic ring, CH_3 (up) of the terminal methyl and CH_2 (down).

The COSY (H-H correlation spectroscopy) spectrum (figure 4.12) provided the proton-proton connectivity network. This spectrum further strengthened the discussions made on the ^{1}HNMR spectrum of this compound. Figure 4.13 showed the HETCOR (heteronuclear chemical shift correlation) spectrum of compound A. This spectrum identified the protons directly bound to the carbon atoms. From this spectrum, it could be deduced that the proton signal centered at 7.31 ppm were attributable to the H-6, H-7 and H-8, while those centered at 7.46 ppm were attributable to H- 5 and H-9. The HMBC (heteronuclear multiple bond connectivity) spectrum depicted in figure 4.12 gave information on heteronuclear shift correlation via long-range C-H couplings (7-10 Hz) usually from ^2J and ^3J. HMBC spectra are useful for complete structural assignments. The long-range correlation as shown in figure 4.14 further supported the discussions made on the preceeding spectrums.

Consequently, comparison of the empirical data with the literature values of a known compound brought to the conclusion that compound A was ethyl cinnamate **83**[23,116,117].

FIGURE 4.11 DEPT SPECTRUM OF COMPOUND A

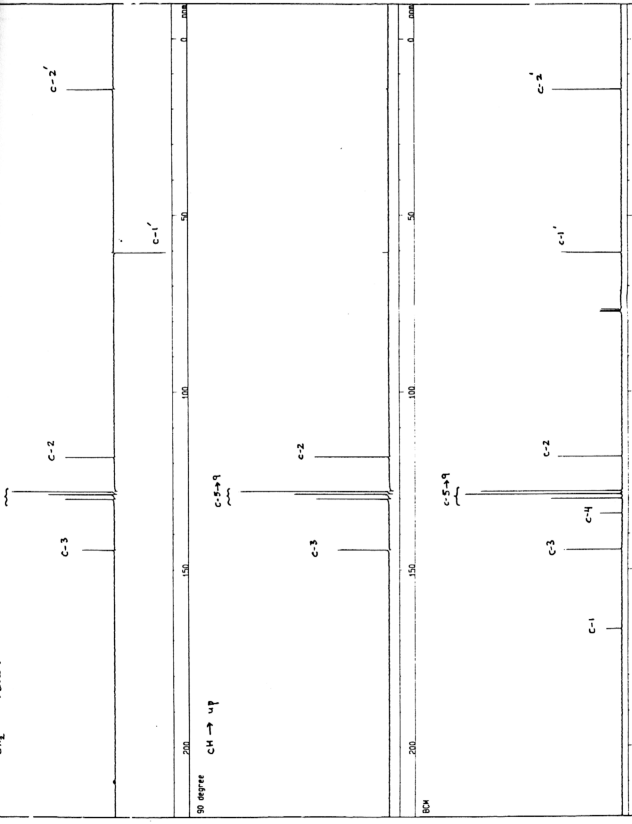

FIGURE 4.12 COSY SPECTRUM OF COMPOUND A

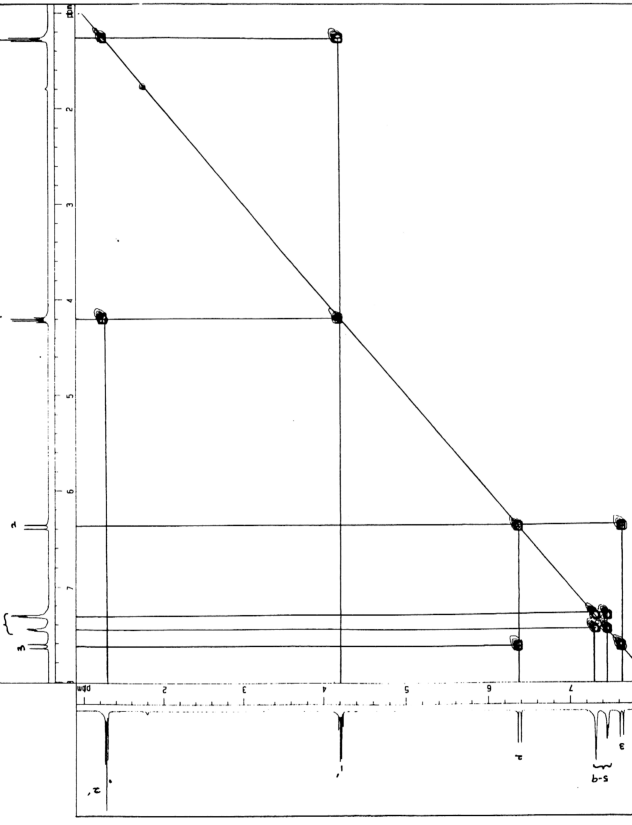

FIGURE 4.13 HETCOR SPECTRUM OF COMPOUND A

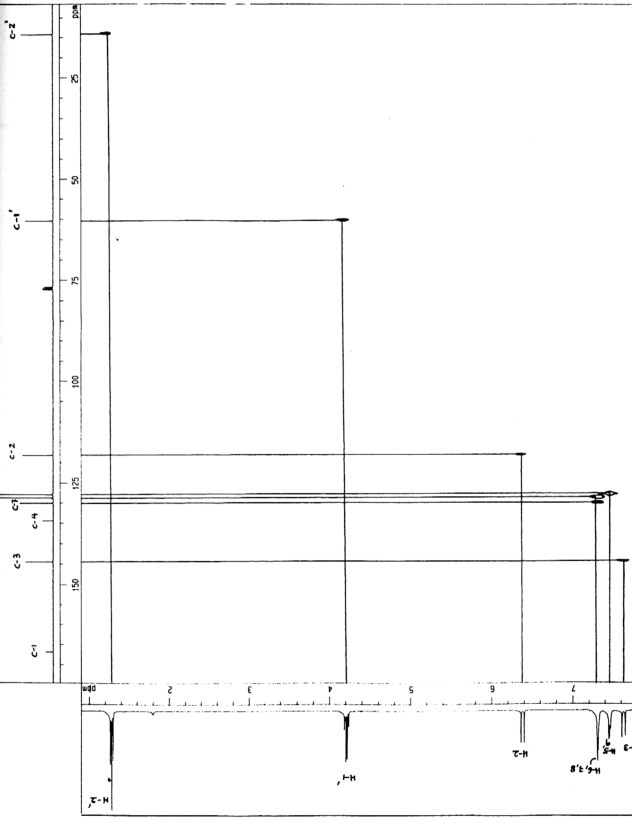

FIGURE 4.14 HMBC SPECTRUM OF COMPOUND A

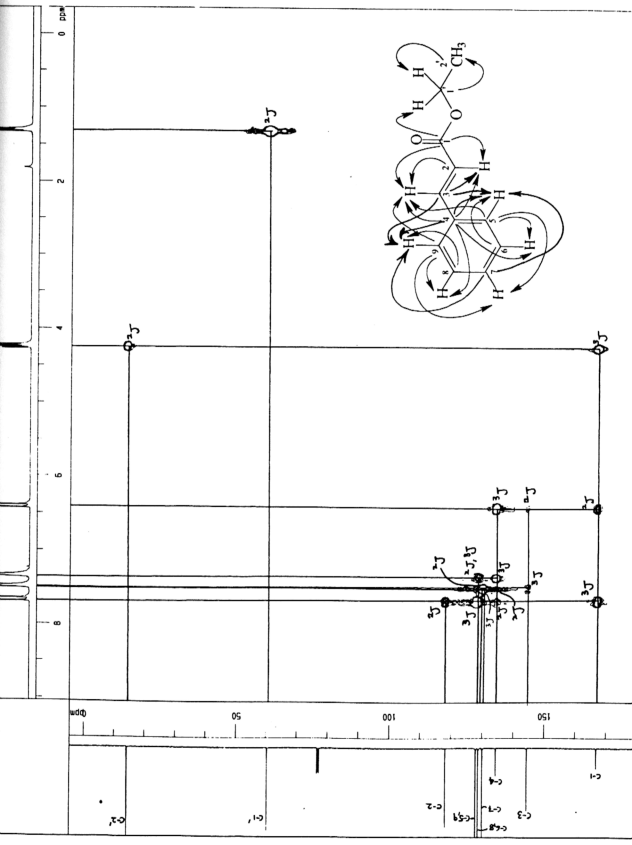

4.1.4.2 *Compound B*

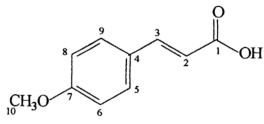

84

Compound B was isolated as white needles with melting point of 176-177°C. It's UV spectrum revealed a broad band containing multiple peaks between 218.3 nm (log ε 4.04) and 309.6 nm (4.15), and a peak at 290.2 nm (4.21), indicating a highly unsaturated chromophoric system.

The IR spectrum of compound B (figure 4.15) revealed a broad, intense O–H (of an acid) stretching absorption in the region of 3049 - 2594 cm^{-1} [65]. The aryl, alkenyl and alkyl C–H stretching at 3049, 3000, 2964 and 2841 cm^{-1} were superimposed upon the O–H stretching. In addition, the band at 1687 cm^{-1} could be assigned to the stretching vibrations of the conjugated C=O bond (i.e. α,β-unsaturated acid conjugated with an aromatic ring[68]), while that at 1428 cm^{-1} to the C–O–H in-plane bending. Meanwhile, the peaks at 1603 and 1513 cm^{-1} could be due to C=C bond stretching of the benzene ring and alkene. Lastly, the strong peak at 1255 cm^{-1} could be due to the asymmetrical stretching of C-O-C of the aryl alkyl ether.

FIGURE 4.15 IR SPECTRUM OF COMPOUND B

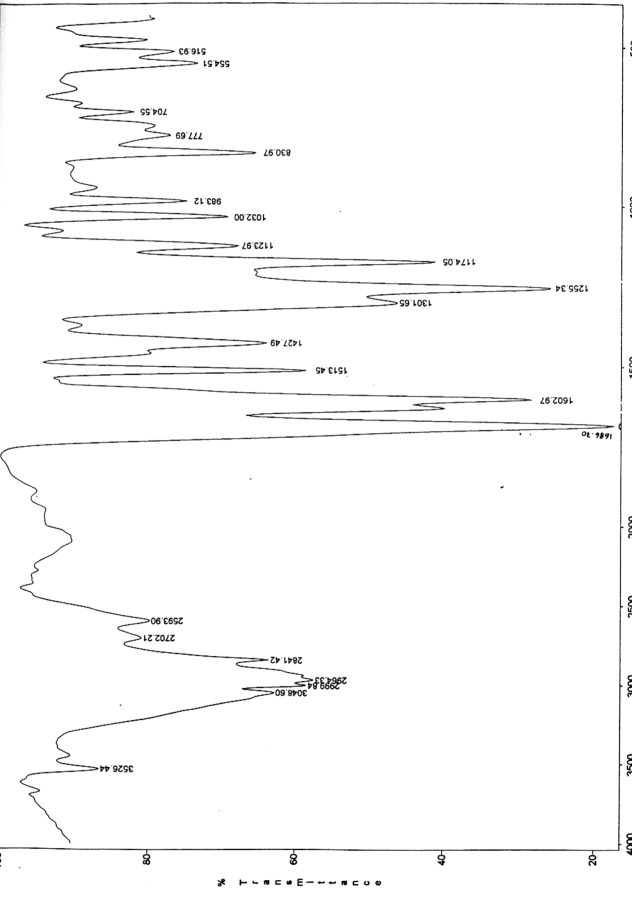

The mass spectrum (figure 4.16) exhibited a molecular ion peak which was also the base peak (100%) at m/z = 178, thus giving the possibility of the molecular formula to be $C_{10}H_{10}O_3$. Peaks were also observed at m/z = 161 and 133 suggesting the loss of a hydroxyl and a carbonyl, respectively. Scheme 4.2 illustrates the proposed fragmentation patterns of compound B.

The ^{1}HNMR spectrum of compound B clearly showed the presence of two AX systems; protons of the ethylene and the 1,4-disubstituted benzene ring with $\Delta\nu/J \sim 36$ and ~ 27, respectively. From figure 4.17, existence of a doublet at 6.30 ppm (1H, d, J_2 = 15.9 Hz) might be attributed to H-2, while H-3 resonated further downfield at 7.73 ppm (1H, d, J_3 = 15.9 Hz). The deshielding effect on H-3 was due to the fact that it was connected to the carbon situated at a β- position to the acid moiety (refer chapter 4.1.4.1).

A strong peak resonating at 3.82 ppm corresponding to three protons was attributable to the methoxy protons directly attached to the aromatic ring at the *para*- position. The fact that the methoxy group was attached directly to the ring explained the strong anisotropic effect, hence the deshielding effect, experienced by the protons on the methoxy.

The doublet at 6.90 ppm corresponding to two protons (2H, d, $J_6 = J_8$ = 8.8 Hz) belonged to H-6 and H-8, while the doublet at 7.49 ppm (2H, d, $J_5 = J_9$ = 8.8 Hz) could be assigned to two protons, each bonded to C-5 and C-9. The resonations of H-6 and H-8 were more upfield compared to those of benzene protons ($\sim$ 7.27

FIGURE 4.16 MASS SPECTRUM OF COMPOUND B

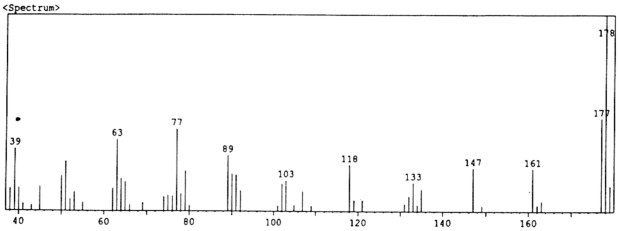

SCHEME 4.2 THE MASS FRAGMENTATION PATTERNS OF COMPOUND B

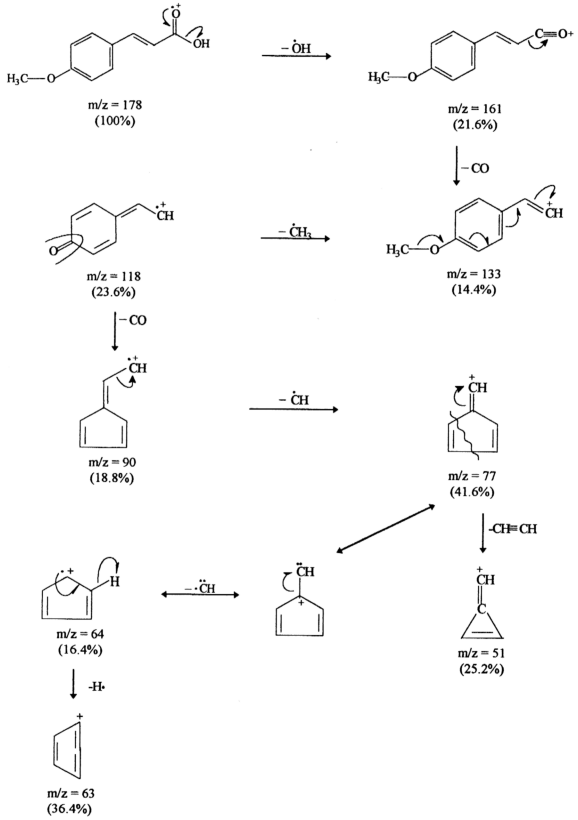

FIGURE 4.17 ^{1}HNMR SPECTRUM OF COMPOUND B

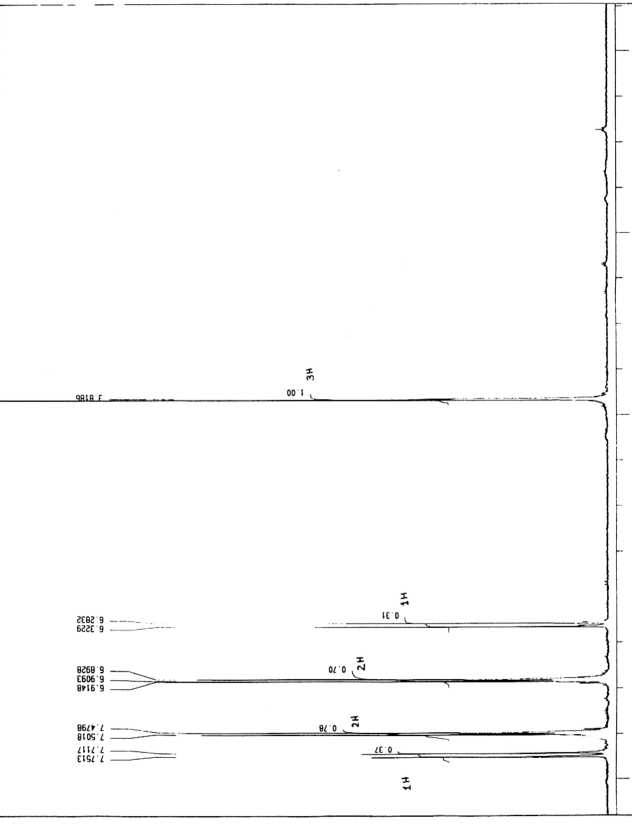

ppm) and this scenario could be explained by the fact that CH_3O is a π-donor and shielding is more prominent on the *ortho-* proton compared to the *meta-* proton[111]. Moreover, the α,β-unsaturated acid moiety bonded to C-4 caused deshielding effect more prominently on H-5 and H-9 compared to H-6 and H-8, thus the downfield signals of H-5 and H-9.

The signal for the acid proton of compound B could not be seen in figure 4.14. This might be because the peak was too broad to be recorded as a sharp signal. In usual cases, carboxylic protons absorb in a characteristically narrow range between ~13.2 - ~10.0 ppm, and the peak widths range from sharp to broad, depending on the exchange rate of the particular acid[65]. Nevertheless, the presence of the carboxylic proton was shown in the IR spectrum.

The ^{13}CNMR spectrum (figure 4.18) showed a signal at 55.40 ppm corresponding to the methoxy carbon attached to the aromatic ring. The peak at 114.43 ppm could be assigned to C-6 and 8 (the theoretical calculated value, $\delta_{C6,8}$ = 112 ppm), while that at 130.11 ppm to C-5 and 9 ($\delta_{C5,9}$ = 127.6 ppm). The peaks at 161.79 (δ_{C7} = 155.2 ppm) and 172.30 ppm might be attributable to the quarternary carbons, C-7 and C-1, respectively. In addition, the sp^2 carbon at position 3 resonated at 146.74 ppm. However, the signals at 114.64 and 126.85 ppm could each be due to either C-2 or C-4; since the theoretical calculated value of the chemical shift of C-4 is 128 ppm, it could be suggested that the signal at 126.85 ppm belonged to C-4.

FIGURE 4.18 ^{13}CNMR SPECTRUM OF COMPOUND B

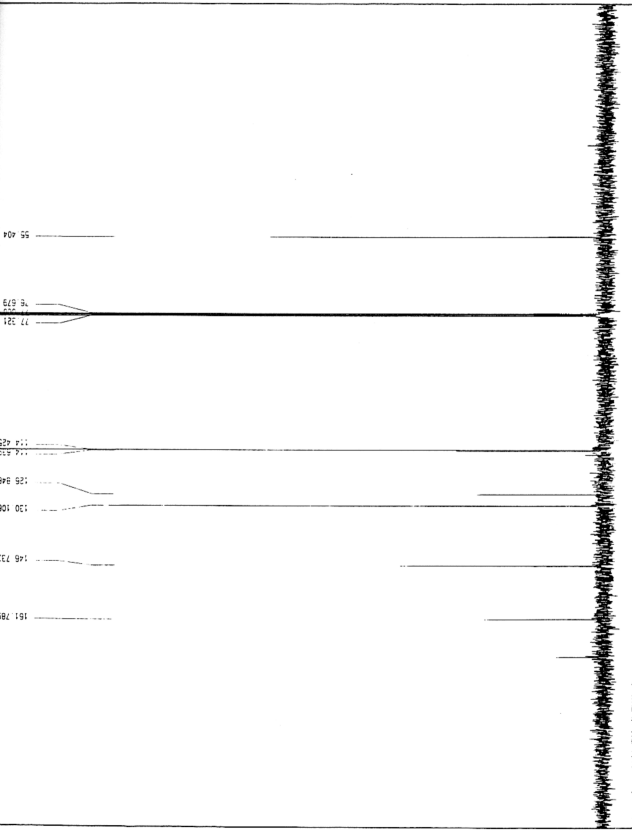

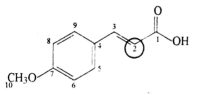

$\delta_{C2} = (123.3 + 6.3 - 11.0)$ ppm = 118.6 ppm

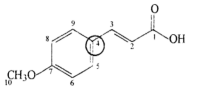

$\delta_{C4} = (128.5 + 7.6 - 8.1)$ ppm = 128.0 ppm

Figure 4.19 showed the DEPT spectrum of compound B. This spectrum distinguished the C, CH and CH_3 signals present in this compound. Figure 4.20 showed the COSY spectrum of compound B and this further supported the proton assignments from the ^{1}HNMR spectrum. From the HETCOR spectrum (figure 4.21), the C-H correlation showed that the peak at 114.64 ppm in the ^{13}CNMR spectrum belonged to C-2, while the peak at 126.85 ppm belonged to the quartenary carbon at position 4. The HMBC spectrum illustrated in figure 4.22, showed the long-range C-H couplings in compound B. Hence the complete assignments of this compound were achieved.

As a result, with comparison of the spectroscopic data obtained from compound B and the literature, the former was confirmed to be *p*-methoxycinnamic acid **84**.

FIGURE 4.19 DEPT SPECTRUM OF COMPOUND B

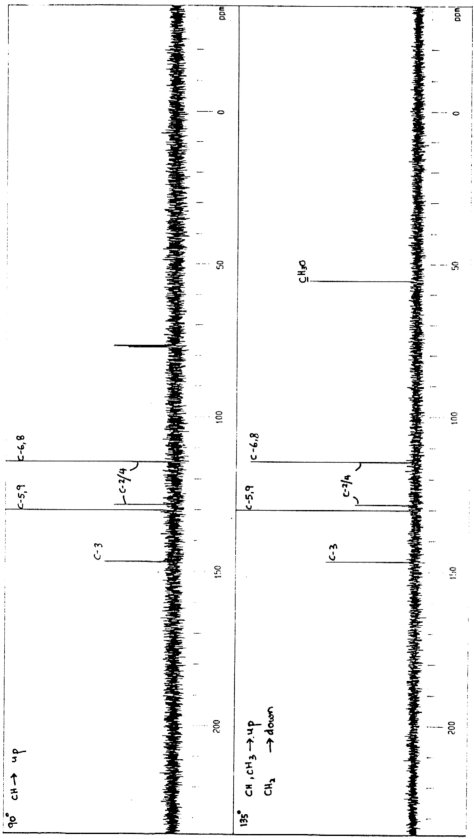

FIGURE 4.20 COSY SPECTRUM OF COMPOUND B

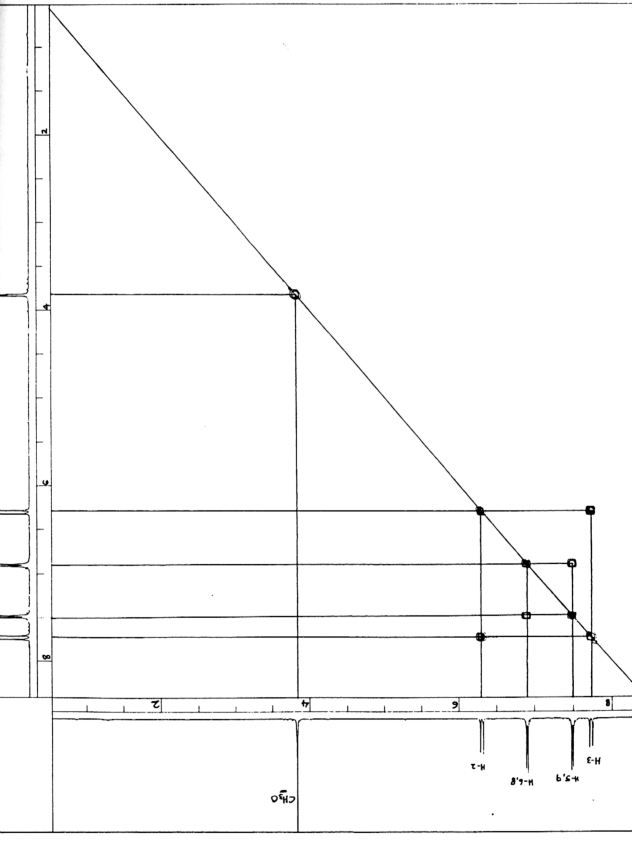

FIGURE 4.21 HETCOR SPECTRUM OF COMPOUND B

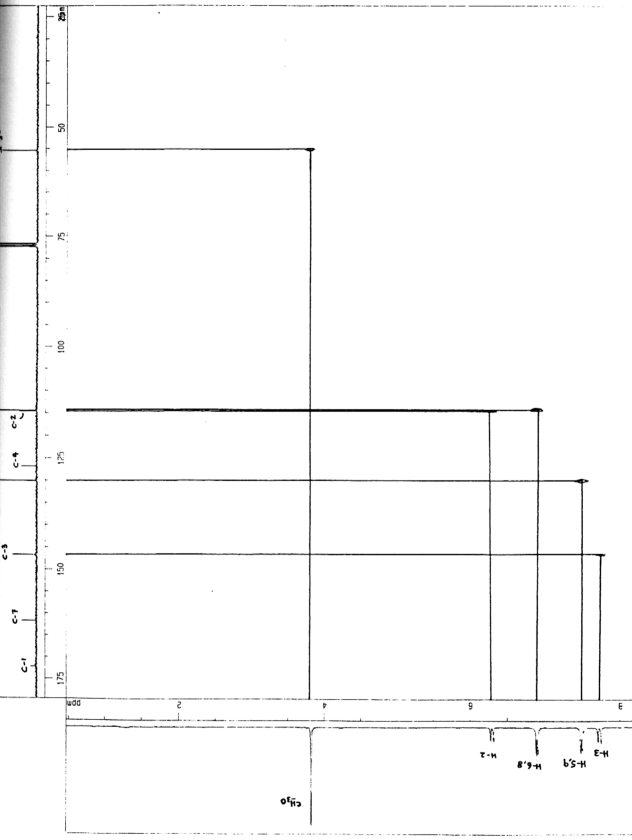

FIGURE 4.22 HMBC SPECTRUM OF COMPOUND B

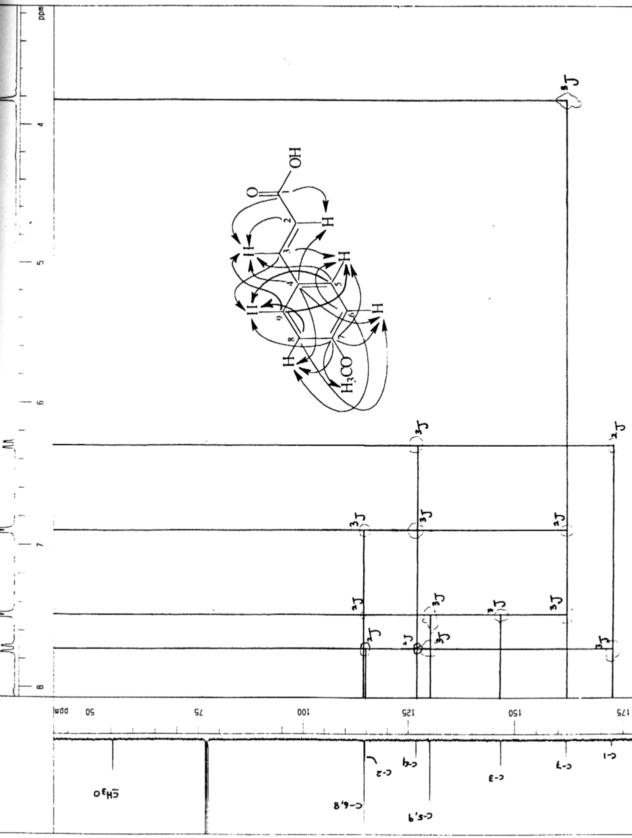

4.2 CHEMICAL STUDY OF THE PET. ETHER EXTRACT OF *KAEMPFERIA GALANGA* LINN.

In this study, sixty-two volatile components of *Kaempferia galanga* L. were identified from the pet. ether extract using the GC-MS. In addition compound C was crystallized from the pet. ether extract under cold condition. Purification of compound C was carried out by recrystallization from pet. ether (40° - 60°C) to produce clear, colourless prisms which represented 50.21% of the crude pet. ether extract.

4.2.1 Structural elucidation and determination of compounds isolated from the pet. ether extract of *Kaempferia galanga* Linn.

4.2.1.1 *Volatile components of Kaempferia galanga* Linn.

The volatile components of *Kaempferia galanga* Linn. were obtained from the pet. ether extract and analysed using gas chromatography - mass spectrometer (GC-MS). The components were confirmed against standard compounds and comparisons were made with standard NIST library. Figure 4.23 shows the gas chromatogram of the volatile components and table 4.3 lists the components and their percentage amounts. From the table, the major compounds were found to be ethyl cinnamate (23.16 %) and *n*-pentadecane (42.63 %) with retention times (Rt) of 19.95 and 21.82 minutes, respectively. Besides phenolics, the volatile components also consisted of several terpenes.

FIGURE 4.23 GAS CHROMATOGRAM OF VOLATILE COMPONENTS OF *KAEMPFERIA GALANGA* LINN.

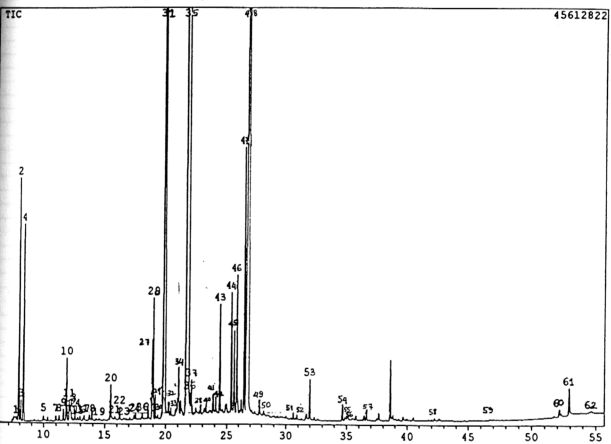

TABLE 4.3 VOLATILE COMPONENTS OF *KAEMPFERIA GALANGA* ELUCIDATED FROM GC-MS

k No	Rt	Mol. Formula	%	Name
	7.692	$C_9H_{16}O$	0.09	2-Nonyn-1-ol
	7.900	$C_{10}H_{16}$	1.61	3-Carene
	8.075	$C_{10}H_{14}$	0.17	1,3,8-p-methatriene
	8.292	$C_{10}H_{18}O$	1.57	Cineol @ eucalyptol
	9.225	$C_9H_{20}O$	0.06	n-Nonal-1-ol
	9.975	$C_{10}H_{16}O_2$	0.07	Trans,trans-octa-2,4-dienyl acetate
	10.992	$C_{12}H_{20}O_2$	0.14	Dihydrocarveol acetate
	11.267	$C_{12}H_{18}$	0.07	8-Methylenedispiro-2.1.2.4-undecane
	11.600	$C_{10}H_{18}O$	0.13	Myrcenol
	11.867	$C_{10}H_{18}O$	0.59	(-)-Borneol @ Borneol
	12.083	$C_{10}H_{14}O$	0.19	p-Cymen-8-ol
	12.150	$C_{12}H_{14}O_2$	0.09	3-Cyclohexen-1-ol,5-methylene-6-(1-methylethenyl)-,acetate.
	12.192	$C_{10}H_{14}O$	0.19	p-Cymen-8-ol
	12.542	$C_{10}H_{18}O$	0.14	Terpenol
	12.873	$C_{10}H_{18}O$	0.06	4-Ethyl-1,4-dimethyl-2-cyclohexen-1-ol
	12.967	$C_{10}H_{16}O$	0.09	Umbellulol @ 3-Thujen-2-ol,stereoisomer
	13.300	$C_8H_{14}O$	0.09	Methyl heptanone
	13.725	$C_8H_8O_2$	0.10	Aubepine @ 4-Methoxybenzaldehyde
	14.533	$C_{12}H_{20}O_2$	0.07	p-Menth-8-en-2-ol,acetate @ Dihydrocarvyl acetate
	15.492	$C_{10}H_{14}O$	0.44	D-Verbenone @ (+)-Verbenone
	15.842	$C_{10}H_{16}O_2$	0.08	Limonene diepoxide
	16.250	$C_{11}H_{24}$	0.13	Undecane
	16.592	$C_{13}H_{22}O$	0.05	Solanone
	17.458	$C_{10}H_{18}O$	0.14	(-)-cis-Sabinol @ 4(10)-Thujen-3-ol, stereoisomer
	17.600	$C_{12}H_{20}O_2$	0.09	Dihydrocarvyl acetate
	18.133	$C_{15}H_{24}$	0.09	α-Cubebene
	18.917	$C_{15}H_{24}$	0.73	α-Gurjunene
	19.008	$C_{14}H_{30}$	1.01	n-Tetradecane
	19.175	$C_{15}H_{24}$	0.28	α-Guaiene
	19.367	$C_{12}H_{18}$	0.09	1-(2-methylene-3-butenyl)-1-(1-methylenepropyl)cyclopropane
	19.950	$C_{11}H_{12}O_2$	23.16	Ethyl cinnamate
	20.258	$C_{15}H_{24}$	0.12	α-Humulene @ α-Caryophyllene
	20.450	$C_{15}H_{24}$	0.07	(1.α.,3.α.,5.α.)-(1,5-diethenyl-3-methyl-2-methylene)-Cyclohexane
	21.225	$C_{15}H_{26}$	0.20	Patchoulane
	21.817	$C_{13}H_{22}$	42.63	n-Pentadecane
	21.975	$C_{15}H_{24}$	0.31	cis-(-)-2,4a,5,6,9a-hexahydro-3,5,5,9-tetramethyl-(1H)-benzocycloheptene
	22.100	$C_{15}H_{26}O$	0.40	8-Cadinol
	22.842	$C_{15}H_{24}$	0.10	trans-Caryophyllene
	23.133	$C_{14}H_{22}$	0.11	12-methyl-[E,E]-1,5,9,11-Tridecatetraene
	23.283	$C_{13}H_{22}$	0.11	(E)-3-Tridecen-1-yne
	23.875	$C_{15}H_{24}O$	0.24	1R-(1R@,3E,7E,11R@)-(1,5,5,8-tetramethyl)-(12-oxabicyclo-9.1.0-dodeca-3,7-diene
	24.100	$C_{14}H_{30}$	0.14	Isotetradecane
	24.433	$C_{17}H_{14}O_3$	1.25	2-Propenoic acid,3-(4-methyoxyphenyl)-ethyl ester
	25.400	$C_{10}H_{16}O_2$	1.28	2,7-Octadien-1-ol,acetate,(Z)-
	25.633	$C_{16}H_{30}$	1.09	7-Hexadecyne
	25.867	$C_{17}H_{34}$	1.84	8-Heptadecene
	26.492	$C_{14}H_{30}$	2.88	n-Tetradecane @ isotetradecane
	26.850	$C_{12}H_{14}O_3$	8.28	Ethyl 3-(4-methoxy)phenyl- 2-propenoate
	27.817	$C_{16}H_{34}O$	0.18	Hexadecanol
	28.167	$C_{20}H_{40}O_2$	0.07	Methyl 4,6,10,14-tetramethyl-pentadecanoate
	30.608	$C_{11}H_{22}O_2$	0.06	n-Nonyl acetate
	30.908	$C_{10}H_{11}N_3O_5$	0.06	N-(2,4-dinitrophenyl)morpholine
	31.983	$C_{22}H_{40}O_2$	0.43	2-(7-heptadecynyloxy)tetrahydro-2H-pyran
	34.658	$C_{17}H_{24}O$	0.17	Falcarinol(Z)-(-)-1,9-heptadecadiene-4,6-diyne-3-ol
	34.883	$C_{16}H_{18}O$	0.08	9-Decyn-1-ol
	35.050	$C_{10}H_{20}O$	0.07	Trans-3-decen-1-ol
	36.658	$C_{22}H_{40}O_2$	0.13	2-(7-heptadecynyloxy)tetrahydro-2H-pyran
	42.242	$C_{23}H_{40}O_4$	0.07	(Z,Z,Z)-2,3-bis(acetyloxy)propyl-9,12,15-octadecatrienoate
	46.733	$C_{11}H_{10}O_4$	0.01	3,7-Dimethoxycoumarin
	52.167	$C_{10}H_{14}N_2$	0.12	2-Butyl-2-methyl-1,1-cyclopropanedicarbonitrile
	52.925	$C_{25}H_{40}O_6$	0.38	(Z,Z,Z)-2-(acetyloxy)-1-(acetyloxy)methyl ethyl-9,12,15-Octadecatrienoate
	54.642	$C_{15}H_{30}O$	0.06	2-Pentadecyn-1-ol

4.2.1.2 *Compound C*

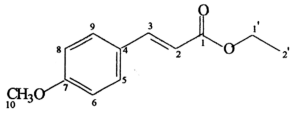

58

Compound C was obtained as colourless prisms with melting point of 48-49°C. The mass spectrum (figure 4.24) revealed a molecular ion peak at m/z = 206 allowing the possibility of the molecular formula to be $C_{12}H_{14}O_3$. Other peaks were also observed at m/z = 178, 161 (100%; base peak), 133, 118, 90, 77 and 64. The proposed fragmentation patterns of compound C are as illustrated in scheme 4.3. The compound underwent Mc Lafferty rearrangement to eliminate an ethylene unit giving rise to a peak at m/z = 178. Subsequently, a hydroxyl was lost to give the base peak at m/z = 161. Successive elimination of a carbonyl, a methyl and a carbonyl again consequently revealed a peak at m/z = 90. Then, further losses of two •CH radicals produced a peak at m/z = 64.

It's UV spectrum revealed a broad band containing multiple peaks between 298 nm (log ε 4.35) and 308 nm (4.38), and peaks at 211.4 nm (4.08) and 227.4 nm (4.11), indicating a highly unsaturated chromophoric system.

The IR spectrum of compound C (figure 4.25) revealed a peak at 3033 cm^{-1} which was due to the aromatic C–H stretching. The bands between 3000 and 2908 cm^{-1} were attributable to the C–H stretching of the alkyl and alkene groups, while

FIGURE 4.24 MASS SPECTRUM OF COMPOUND C

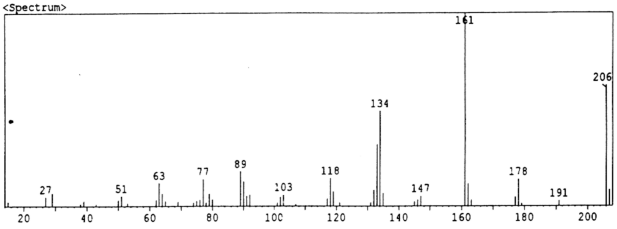

SCHEME 4.3 THE MASS FRAGMENTATION PATTERNS OF COMPOUND C

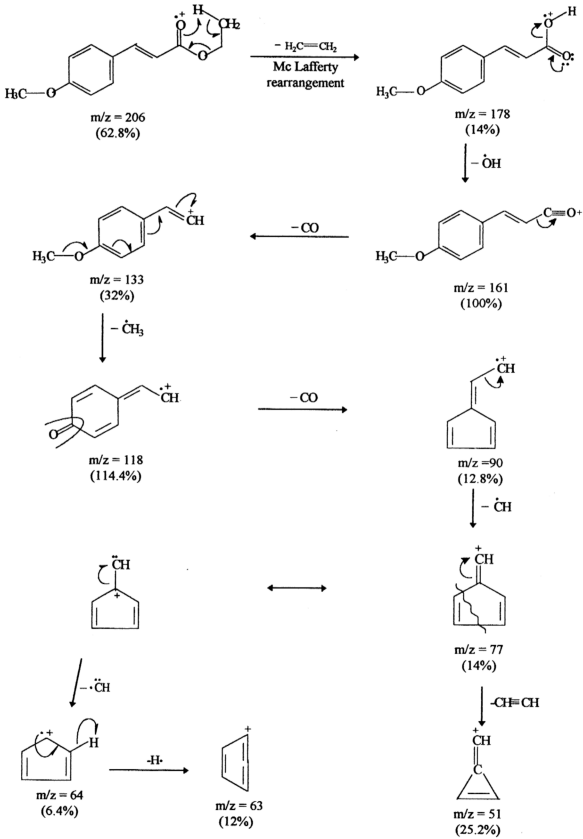

FIGURE 4.25 IR SPECTRUM OF COMPOUND C

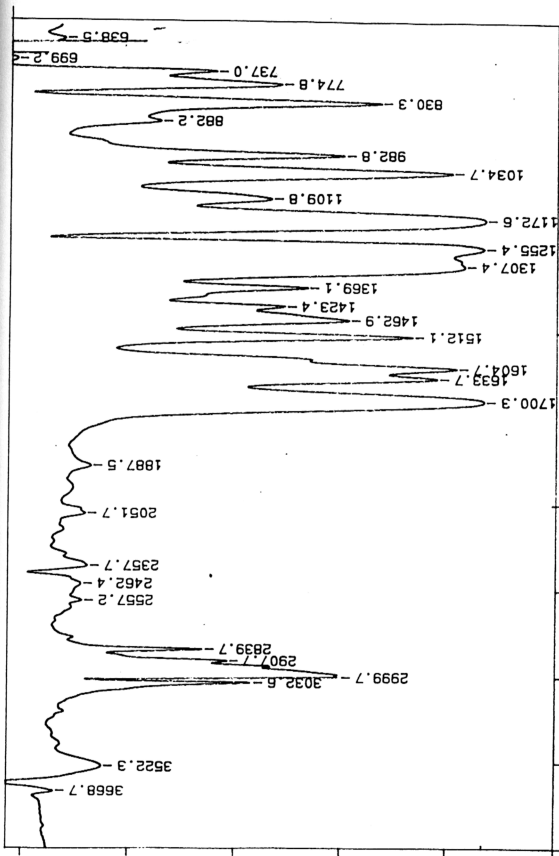

the band at 2840 cm^{-1} could be assigned to the methoxy moiety. Furthermore, the strong band at 1700 cm^{-1} would be due to the stretching vibrations of the conjugated C=O bond (i.e. α,β-unsaturated ester conjugated with the aromatic ring), while the bands between 1634 and 1463 cm^{-1} might be attributable to the C=C stretching. Meanwhile, multiple peaks that could be observed between 1307 and 1255 cm^{-1} could be due to the C–O stretching of the ester moiety (i.e. C–C(=O)–O). In addition, the peaks at 1172 and 1035 cm^{-1} could be assigned to the asymmetrical and symmetrical C–O–C stretching, respectively.

Figure 4.26 revealed the ^{1}HNMR of compound C. From this spectrum, it could be deduced that the triplet corresponding to three protons at 1.32 ppm belonged to a methyl adjacent to an ethyl. A strong peak at 3.81 ppm corresponding to three protons would be due to the methoxy directly attached to the aromatic ring. Meanwhile, a quartet at 4.25 ppm could be assigned to the two protons on the ethyl group, adjacent to the methyl and bonded to an oxygen atom of an ester moiety (hence, explaining the highly deshielding position caused by the neighbouring oxygen atom).

This spectrum also revealed the presence of AX systems on protons of the ethylene and the 1,4-disubstituted benzene ring with $\Delta\nu/J \sim 33$ and 26, respectively. The doublet resonating at 6.31 ppm (1H, d, J_2 = 15.9 Hz) belonged to H-2, while H-3 resonated further downfield at 7.63 ppm (1H, d, J_3 = 16.1 Hz). The strong deshielding effect felt by H-3 was caused by the fact that it was at a β-position to an ester (refer chapter 4.1.4.1).

FIGURE 4.26 ^{1}HNMR SPECTRUM OF COMPOUND C

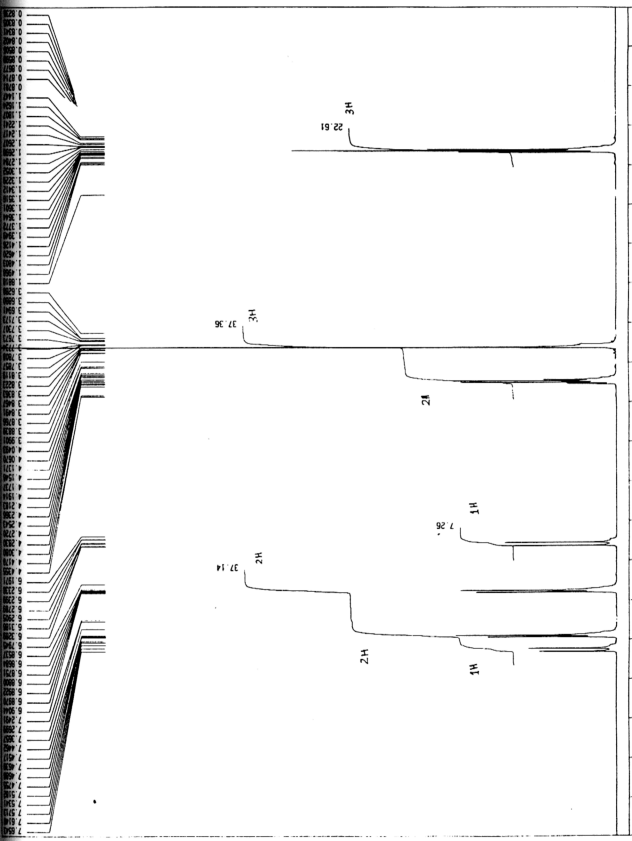

FIGURE 4.27 ^{13}CNMR SPECTRUM OF COMPOUND C

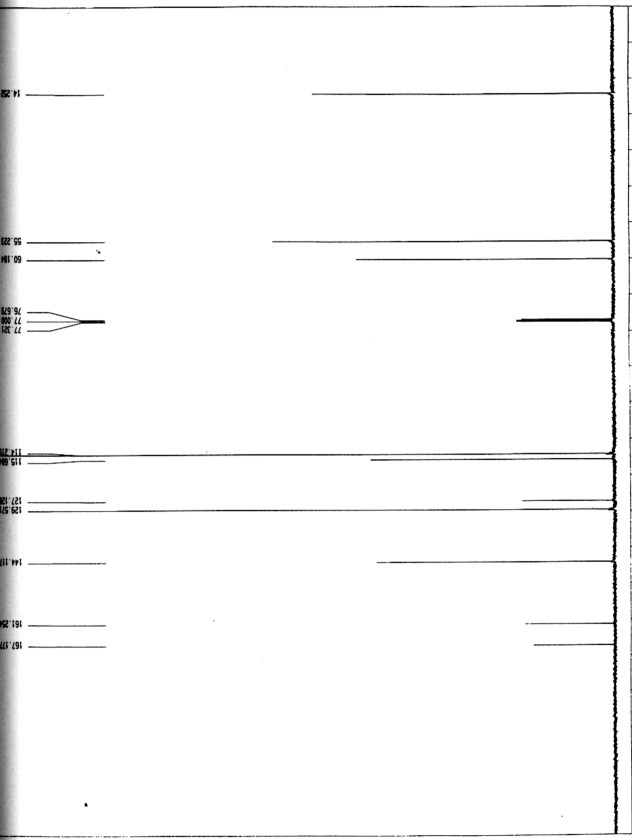

A doublet at 6.89 ppm corresponding to two protons (2H, d, $J_6 = J_8 = 8.8$ Hz) belonged to H-6 and H-8, while the doublet resonating at 7.46 ppm (2H, d, $J_5 = J_9 = 9.0$ Hz) could be assigned to two protons, each bonded to C-5 and C-9.

The ^{13}CNMR spectrum of compound C (figure 4.27) revealed a signal at 14.25 ppm attributable to the methyl carbon adjacent to the ethyl group. Meanwhile, the ethyl carbon adjacent to the methyl and the oxygen atom gave rise to a peak at a downfield position at 60.18 ppm due to the deshielding effect caused by the neighbouring oxygen atom. A signal at 55.22 ppm corresponded to the methoxy carbon which was directly attached to the aromatic ring. The peak at 114.22 ppm could be assigned to C-6 and 8 (the theoretical calculated value, $\delta_{C6,8}$ = 112 ppm), while that at 129.57 ppm to C-5 and 9 ($\delta_{C5,9}$ = 127.6 ppm). The peaks at 161.25 (δ_{C7} = 155.2 ppm) and 167.18 ppm might be attributable to the quarternary carbons, C-7 and C-1, respectively. In addition, the sp^2 carbons at position 2 and 3 resonated at 115.68 and 144.12 ppm, respectively. Lastly, the signal at 127.13 ppm (δ_{C7} = 127.6 ppm) could be attributed to C-4.

Figure 4.28 showed the DEPT spectrum of compound C. This spectrum distinguished the C, CH and CH_3 signals present in this compound. Figure 4.29 showed the COSY spectrum of compound C and this further confirmed the proton assignments from the ^{1}HNMR spectrum. From the HETCOR spectrum (figure 4.30), we could see the C-H correlation of compound C. The HMBC spectrum as illustrated in figure 4.31 showed the long-range C-H interactions and thus completed the structural assignments of this compound.

FIGURE 4.28 DEPT SPECTRUM OF COMPOUND C

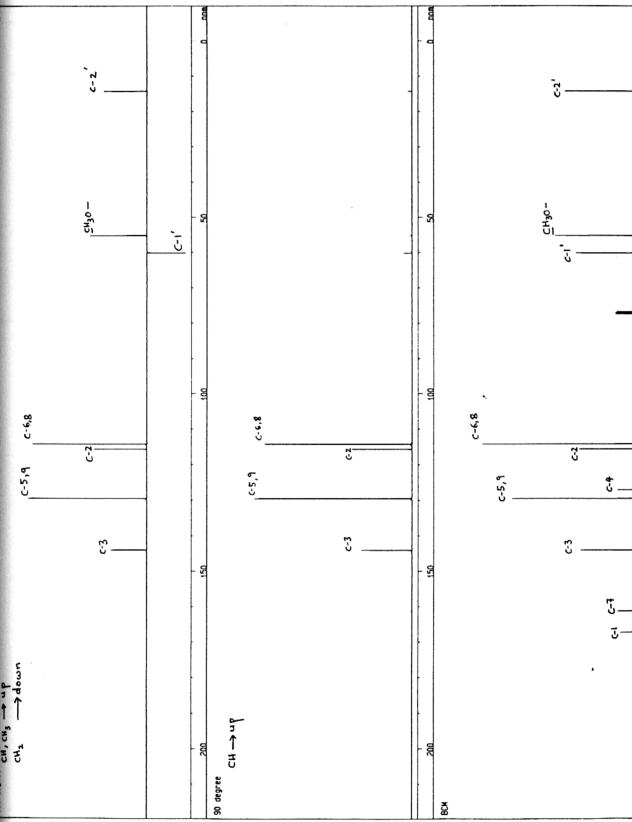

FIGURE 4.29 COSY SPECTRUM OF COMPOUND C

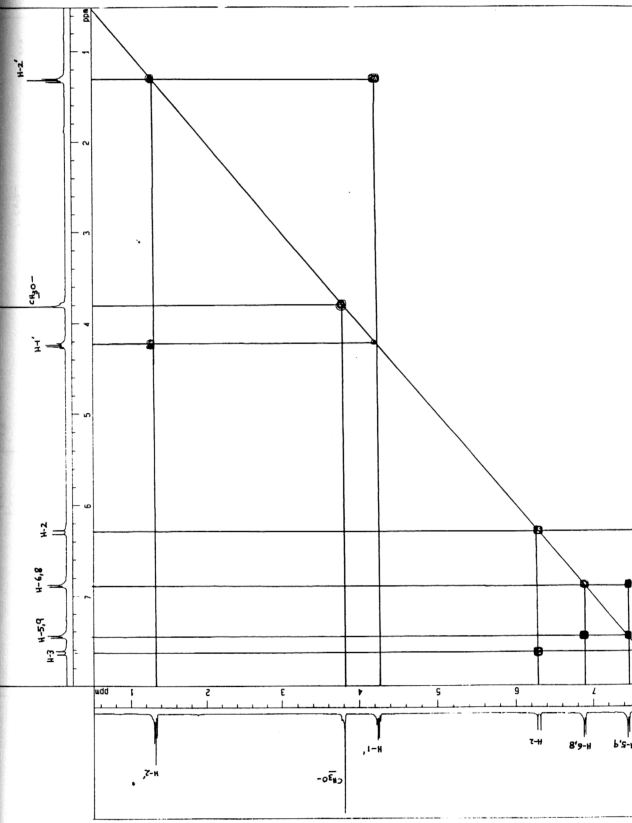

FIGURE 4.30 HETCOR SPECTRUM OF COMPOUND C

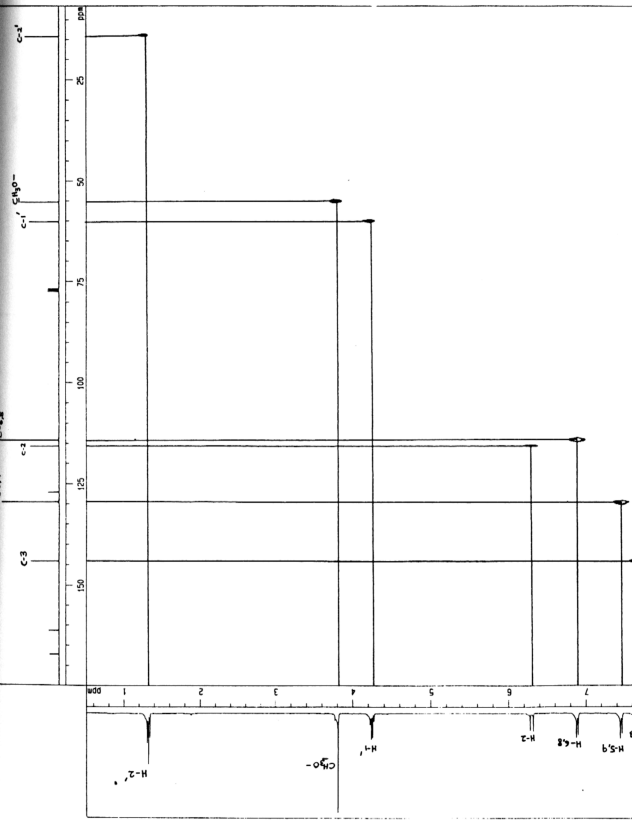

FIGURE 4.31 HMBC SPECTRUM OF COMPOUND C

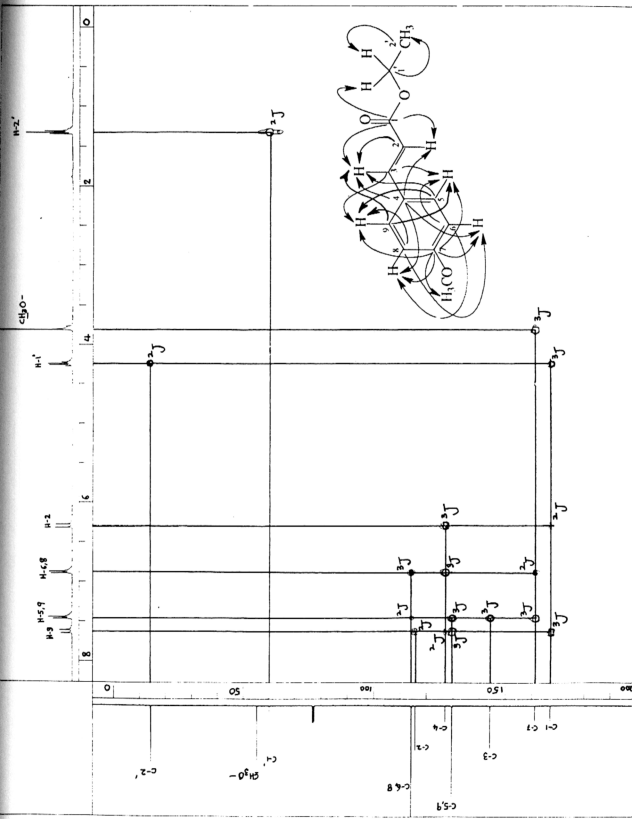

Finally, comparison of the observed data and the literature values of a known compound led to the conclusion that compound C was ethyl *p*-methoxycinnamate **85**.

4.3 MECHANISMS OF VASORELAXANT ACTION OF COMPOUND A AND COMPARISON OF ITS ACTIVITY WITH OTHER STRUCTURALLY SIMILAR COMPOUNDS

In this study, the mechanism of action of compound A on the precontracted rat thoracic aorta was investigated. Compounds B and C exhibited no smooth muscle relaxant activities[118].

Vasorelaxant action of compound A was also compared to several compounds which possessed structurally similar moiety to it, and they are: cinnamaldehyde **86** (labelled as compound D)* , *N*-cinnamalidene-*p*-fluoroaniline **87** (compound E)*, *N*-cinnamalidene-*p*-methoxyaniline **88** (compound F)*, *N*-cinnamalidene-lysin **89** (compound G)*, methyl cinnamate **90** (compound H)** and cinnamyl cinnamate **91** (compound I)**. The relaxant effects of compound A were compared with compounds D to I[119,120].

- *These compounds were kindly contributed by Mr. J. Hidayat and his supervisor, Assoc. Prof. Dr. H. M. Ali.
- **These compounds were purchased from TCI, Japan.

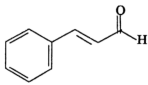

compound D
86

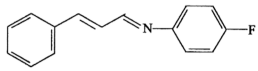

compound E
87

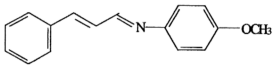

compound F
88

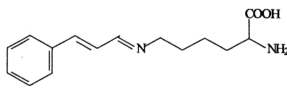

compound G
89

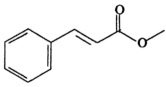

compound H
90

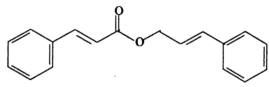

compound I
91

4.3.1 Effects of compound A and related compounds on the contractions induced by high K^+ and PE in endothelium intact rat aorta

As mentioned in section 4.1.3.1, addition of high K^+ to the rat aorta caused a tonic contraction whilst addition of PE caused an initial phasic contraction followed by a tonic contraction. In this experiment, the rat aorta was precontracted with 80 mM of high K^+ or 0.1 μM PE. When contractions to either spasmogens reached maximum, cumulative concentrations of the compounds were added to the bath every ten minutes.

From figures 4.32(a) and 4.32(b), it can be seen that all the compounds exhibited relaxant effects against contractions induced by both high K^+ and PE. Compound A was the most potent inhibitor of the contractions induced by both spasmogens, followed by compounds D, G, H, I, F and E (table 4.4). There were no significant differences in the relaxant activities of compounds A, F and G against the contractions induced by either spasmogens ($p > 0.05$). However, compounds D, H and I exhibited more potent relaxant activities against contractions induced by high K^+ than PE. The relaxant activity of compound E against contractions induced by both spasmogens was quite low since its IC_{50} value could not be determined from the graph.

The results suggested that compounds A, F and G might inhibit Ca^{2+} influx via both VDC and ROC with similar potency, whilst compounds D, H and I were more potent inhibitors of the VDC.

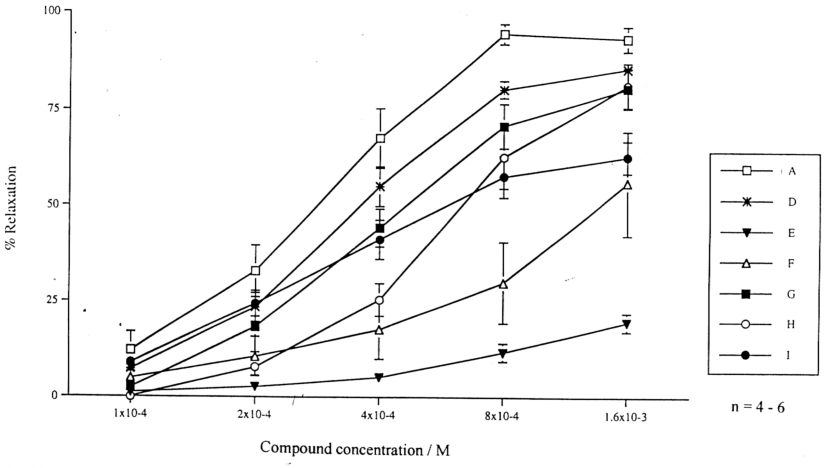

FIGURE 4.32(a) **EFFECTS OF COMPOUND A AND RELATED COMPOUNDS ON THE CONTRACTIONS INDUCED BY HIGH K^+ IN ENDOTHELIUM INTACT RAT AORTA**

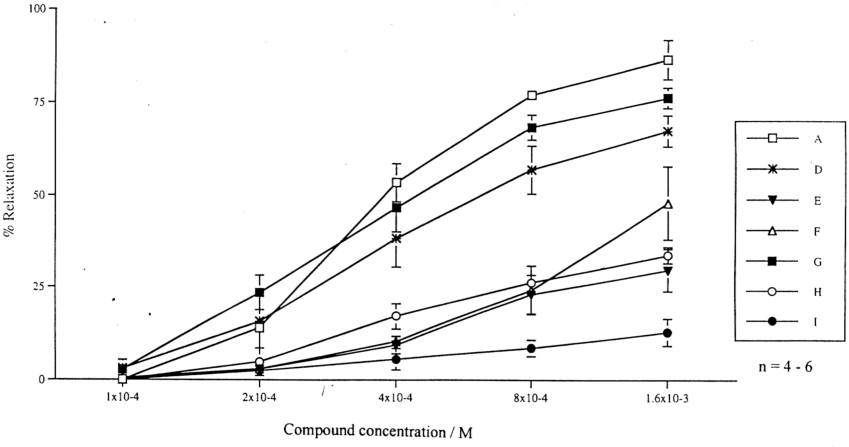

FIGURE 4.32(b) EFFECTS OF COMPOUND A AND RELATED COMPOUNDS ON THE CONTRACTIONS INDUCED BY PE IN ENDOTHELIUM INTACT RAT AORTA

TABLE 4.4 IC_{50} VALUES OF COMPOUNDS A - I FOR THEIR VASORELAXANT ACTIVITIES

	IC_{50} / mM	
Compounds	**High [K^+]**	**Phenylephrine**
A	0.30 ± 0.05	0.38 ± 0.04
D	0.39 ± 0.04 *	0.77 ± 0.20
E	-	-
F	0.94 ± 0.20	1.44 ± 0.20
G	0.49 ± 0.80	0.46 ± 0.07
H	0.67 ± 0.05	-
I	0.62 ± 0.06	-

* : $P < 0.05$ - significant (comparing high [K^+] against PE-induced contractions).

n = 4 - 6

Contractions induced by high K^+ are due to membrane depolarization, which activates L-type VDC and permits Ca^{2+} entry while receptor agonists such as PE activates ROC to induce the sustained contractions. Calcium channel blockers such as verapamil **56** are thought to bind directly to these channels and strongly inhibit Ca^{2+} entry[83]. The present findings that both high K^+- and PE-induced contractions were strongly inhibited dose-dependently by ethyl cinnamate and the structurally similar compounds suggested that the main inhibitory effects of the compounds were due to inhibition of Ca^{2+} influx through these channels.

For the following experiments, the author decided to exclude compounds E, F, H and I since their vasorelaxant activities were rather weak.

4.3.2 Time course of the inhibitory effects of compound A and related compounds on the contractions induced by high K^+ and PE in endothelium intact rat aorta

The aorta was precontracted with 80 mM of high K^+ or 0.1 μM PE as indicated above. When the contractions to either spasmogens became maximum, a single concentration of the compounds A, D or G (based on the IC_{50} values) were added to the bath respectively. From figure 4.33, it can be seen that the rate of relaxation of the high K^+- and PE-induced contractions by compounds A and D were quite similar and more rapid than compound G. The time course of the relaxant activity of the drugs was in good agreement with their order of potency against the contractions induced by both spasmogens. In addition, the IC_{50} of each compound was reached faster in its action against high K^+- than PE-induced contractions

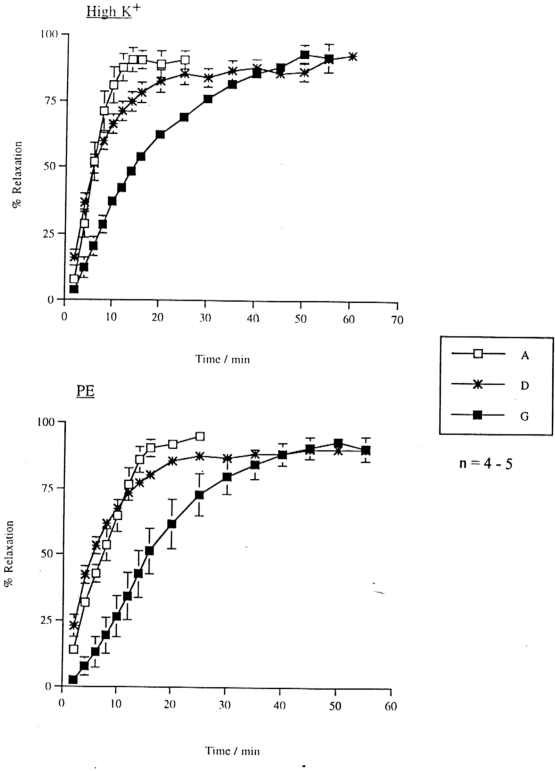

FIGURE 4.33 TIME COURSE OF THE INHIBITORY EFFECTS OF COMPOUND A AND RELATED COMPOUNDS ON THE CONTRACTIONS INDUCED BY HIGH K^+ AND PE IN ENDOTHELIUM INTACT RAT AORTA

respectively: compound A, 5.6 and 8.8 minutes; compound D, 5.6 and 6.4 minutes; compound G, 14.4 and 18 minutes.

4.3.3 Effects of compound A and related compounds on the PE-induced transient contractions of the rat aorta

Although inhibition of Ca^{2+} influx appeared to be the major mechanism of the direct relaxant effect of ethyl cinnamate and compounds D and G, other actions might be involved as it had been shown that most of the Ca^{2+} channel blockers have additional intracellular sites of action[125]. In Ca^{2+}-free Krebs solution (i.e. in the absence of external Ca^{2+}), PE (0.1 μM) induces a rapid transient contraction. PE activates α-adrenoceptor and subsequently stimulates inositol triphosphate (IP3) which then leads to the release of Ca^{2+} from the intracellular stores to mediate the transient contractions[94,122].

In this experiment, compounds A, D and G were preincubated with the rat aorta for 10 minutes prior to the addition of PE to the Ca^{2+}-free solution. Figure 4.34 shows that all the compounds reduced the PE-induced transient contractions in the following order : compounds D (100 ± 0.00%) > A (49.03 ± 4.76%) > G (24.43 ± 3.00%). This finding suggested that all the three compounds variably inhibit Ca^{2+} release from the intracellular stores.

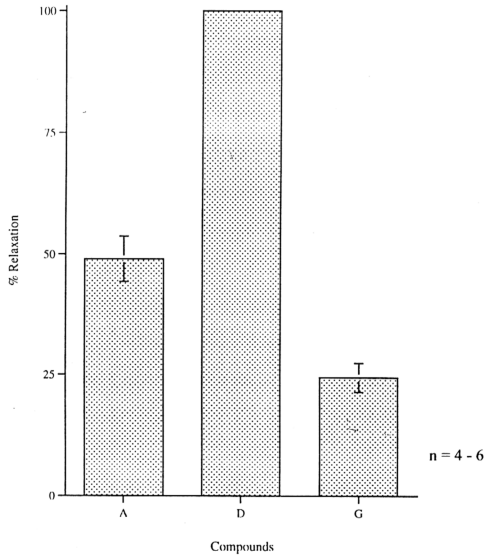

FIGURE 4.34 EFFECTS OF COMPOUND A AND RELATED COMPOUNDS ON THE PE-INDUCED TRANSIENT CONTRACTIONS OF THE RAT AORTA

4.3.4 Effects of compound A and related compounds on the contractions induced by PE in endothelium intact and denuded preparations of the rat aorta

The relaxant actions of compounds A, D and G against PE-induced contractions were compared between endothelium intact and denuded preparations of the rat aorta. The endothelium was removed by gently rubbing the internal wall of the muscle with a blunt forcep. Following the removal of the endothelium, the inhibitory actions of compounds A, D and G against contractions of the aorta were markedly attenuated (figure 4.35). It therefore appears that endothelium-derived relaxant factors (EDRF) or prostacyclins might be partly involved in mediating the relaxant actions of these compounds. The experiment below was designed to investigate this possibility.

4.3.5 Effects of methylene blue and indomethacin on the relaxant actions of compound A and related compounds on the contraction induced by PE in the endothelium intact rat aorta

EDRF activates soluble guanylate cyclase of vascular smooth muscle, and the resulting increase in cyclic GMP levels produces relaxation[121]. Methylene blue is an inhibitor of guanylate cyclase. Indomethacin abolishes the generation of prostacyclins by inhibiting the enzyme cyclo-oxygenase which is involved in the metabolism of arachidonic acid.

In this experiment, the rat aorta was pretreated with methylene blue (10 μM) or indomethacin (20 μM) for 20 minutes before contracting the muscle with 0.1μM

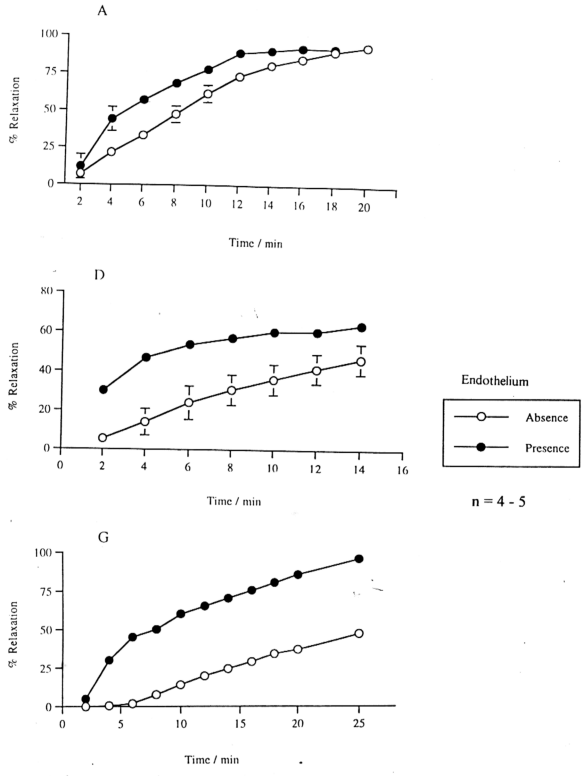

FIGURE 4.35 EFFECTS OF COMPOUND A AND RELATED COMPOUNDS ON THE CONTRACTIONS INDUCED BY PE IN ENDOTHELIUM INTACT AND DENUDED PREPARATIONS OF RAT AORTA

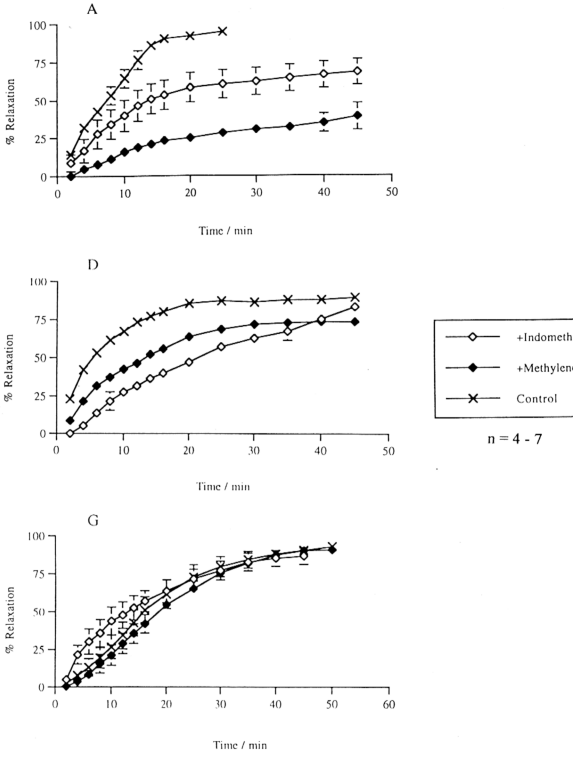

FIGURE 4.36 EFFECTS OF METHYLENE BLUE AND INDOMETHACIN ON THE RELAXANT ACTIONS OF COMPOUND A AND RELATED COMPOUNDS ON THE CONTRACTIONS INDUCED BY PE IN ENDOTHELIUM INTACT RAT AORTA

PE. As shown in figure 4.36, the relaxant effects of both compounds A and D were strongly reduced by pretreatment with methylene blue and indomethacin, confirming the involvement of EDRF and prostacyclin in mediating the actions of the compounds. There was no significant difference in the relaxant action of compound G following pretreatment with indomethacin or methylene blue ($p>0.05$), suggesting that EDRF and prostacyclin were not involved in the relaxant action the compound.

In vascular smooth muscles, sodium nitroprusside **69** (refer section 3.2.4) had been shown to inhibit contraction by decreasing cytosolic Ca^{2+} levels and Ca^{2+} sensitivity of contractile elements[106]. This action of sodium nitroprusside is mediated by activation of guanylate cyclase and subsequent increase in cGMP[126]. The result of the present study suggested that the relaxation effect of *Kaempferia galanga* Linn. was similar to that of sodium nitroprusside as it indirectly involved activation of guanylate cyclase via the release of EDRF.

4.4 CYTOTOXICITY EFFECTS OF COMPOUNDS A AND C ON KB CELLS

In 1985, Kosuge *et. al.* reported the cytotoxic activity of ethyl *p*-methoxycinnamate **85** on HeLa cells (a type of cancer cells) with IC_{50} value of 35 $\mu g\ ml^{-1}$. In this study, compounds A and C were subjected to cytotoxicity tests on another type of cancer cells, i.e. the KB cells. Figure 4.37 illustrates the mortality curves of compounds A and C.

FIGURE 4.37 TOXICITY EFFECTS OF COMPOUNDS A AND C ON KB CELLS

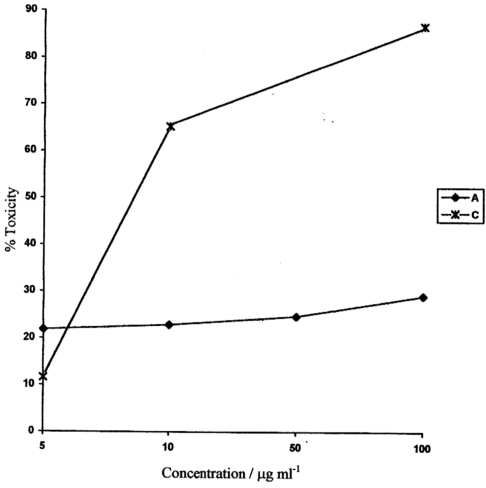

From this figure, it could be deduced that compound A exhibited a very low activity, and the ED_{50} value could not be obtained from the graph. On the other hand, the ED_{50} value of compound C was 8.37 $\mu g\ ml^{-1}$, hence making it mildly active. Plant extracts with $ED_{50} \leq 20\ \mu g\ ml^{-1}$ are considered as active[123].